Improving the Original Dual-T-Snakes Model

GILSON A. GIRALDI[1], EDILBERTO STRAUSS[2], ANTONIO A. F. OLIVEIRA[2]

[1]LNCC–National Laboratory of Scientific Computation - Av. Getulio Vargas, 333, 25651-070 Rio de Janeiro, RJ, Brazil
{giraldi}@lncc.br
[2]LCG–Computer Graphics Laboratory, UFRJ-COPPE - Mail Box 68511, 21945-970 Rio de Janeiro, RJ, Brazil
{strauss,oliveira}@lcg.ufrj.br

Abstract. The Dual-T-Snakes model plus dynammic programming (DP) techniques is an efficient methodology for boundary extraction and segmentation of 2D images. However, the original proposal of the Dual-T-Snakes suffers from difficulties for parameters choise and instabilities due to the normal force definition. Also, the proposed method to push a snake way from a local minimum is not efficient for noise images. In this paper we address these limitations. Firstly, we reduce the number of parameters without affecting the basic features of Dual-T-Snakes. Next, we propose a new normal force definition which maintains the desired features of a balloon-like one but is more stable and gives better performance. Then, we propose other methods to avoid local minima based on mesh resolution, image statistics and a new region growing technique. We demonstrate these methods for artificial and cell images. Finally, in the future works, we figure out how to apply Dual-T-Snakes plus Viterbi together with non-parametric multiscale methods.

1 Introduction

The Dual-T-Snakes is a parametric snake model. Snake models, also called Active Contour Models, are deformable models. They were proposed by Kass at al. [9] and since then have been successfully applied in a variety of problems in computer vision and image analysis, such as edge and subjective contours detection, motion tracking and segmentation [3]. Its mathematical formulation makes easier to integrate image data, an initial estimated, desired contour properties and knowledge-based constraints, in a single extraction process [3].

However, parametric models have also their limitations. First, the topology of the structures of interest must be known in advance since the mathematical model can not deal with topological changes without adding extra machinery [11]. Second, parametric snakes are too sensitive to their initial conditions due to nonconvexity problems [16, 8].

Among the approaches to deal with the topological limitations of the traditional snake model [13], the T-snakes has the advantage of being a general one [12]. On the other hand, to reduce the problems caused by the convergence of a snake to local minima some authors have proposed multiscale methods [10], the addition of other internal force terms [4, 16], as well as Dual Contour approaches [8, 6].

Another way to address the non-convexity problems is based on a two stage approach: (1) the region of interest is reduced; (2) a global minimization technique is used to find the object boundaries. Few works have been done in this direction [2].

In [7] we propose to address the stage (1) by using our Dual-T-Snakes method [7, 5]. The result of this method is two contours close to the object boundary which bound the search space. Hence, a DP algorithm [1, 2, 8] can be used more efficiently.

Despite of the capabilities of Dual-T-Snakes, its practical application has some drawbacks. In this paper we address the corresponding problems and the solutions proposed are the main contribution of this work.

The first point is the parameters choise. We demonstrate that the set of parameters for the original Dual-T-Snakes can be reduced without affecting the fundamental role of this method in our approach: to reduce the search space for DP.

Next, we show that the normal force definition (the same of the T-Snakes model [13]) is inefficient for noise images. A new definition have to be designed to make proper use of the Dual-T-Snakes framework as well as to get better stabilty and performance.

Another important point is the methodology to push a T-Snake away from a local minimum. The original proposal creates instabilities and performance problems for noise images. To address these problem we test three methods: the use of images statistics; change the grid resolution and a new region growing method [5].

Also we demonstrate in section 6 how to use hierarchical filtering and non-linear methods with the Dual-T-Snakes approach. The use of non-parametric multiscale methods in the context of this work is discussed in section 7

The paper is organized as follows. Firstly, we review the T-Snakes model and the Dual-T-Snakes plus DP framework. In section 5 we discuss technical details and present the improvements for Dual-T-Snakes. In section 6 we demon-

1530-1834/01 $10.00 © 2001 IEEE

strate these improvements for syntetic and cell images. Finally, we discuss future works and conclusions.

2 T-Snake: A Framework for Topological Changes

The T-Snakes approach is composed basically by three components [11, 13, 12]: (1) a triangulation (simplicial decomposition) of the domain of interest, in our case a closed subset $D \subset \Re^2$; (2) a particle model of the snake; (3) a *characteristic function* χ defined on the grid nodes which distinguishes the interior from the exterior of an object O:

$$\chi : D \subset \Re^2 \rightarrow \{0,1\} \tag{1}$$

where $\chi(p) = 1$ if $p \in O$ and $\chi(p) = 0$, otherwise.

Following the classical nomenclature, a vertex of a triangle is called a *node* and the collection of nodes and triangle edges is called the (simplicial) grid Γ_s. A triangle σ is a *traverse triangle* if the characteristic function χ in equation (1) changes its value in σ. Analogously, for an edge.

In this framework, the reparameterization of a contour is done by [13, 12]: (1) taking the intersections points of the snake with the triangulation; (2) carrying out topological changes by using the characteristic function χ to distinguishing the inside from the outside of the snake(s).

As an example, consider the characteristic functions (χ_1 and χ_2) relative to the two contours pictured in Figure 1. The functions are defined on the vertices of a CF-triangulation of the plane. The vertices marked are those where $\max\{\chi_1, \chi_2\} = 1$. Observe that they are enclosed by a merge of the contours. This merge can be approximated by a curve belonging to the dual of a two dimensional combinatorial manifold obtained by tracing the boundary triangles [13]. The same would be true for more than two contours (and obviously for only one).

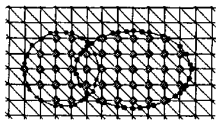

Figure 1: Two snakes colliding with the inside grid nodes and snaxels marked.

2.1 Discrete Snake Model

A T-Snake [13, 12] is a discrete form of the classical snake [9]. It is defined as a set of N particles (*snaxels*), whose positions $\{v_i = (x_i, y_i), i = 0, ..., N-1\}$ are connected to form a closed contour. Each pair of points v_i, v_{i+1} is called a "model element ". The snaxels are linked by springs defined by a stiffness parameter a_i, and a natural length l_i. The corresponding elastic force is added to a rigidity (smoothing) force, a normal (balloon-like) force, and a external (image) force [13, 12]. These forces are given respectively by the following expressions:

$$Elastic\ Force : \alpha_i = a_i e_i r_i(t) - a_{i-1} e_{i-1} r_{i-1}(t). \tag{2}$$

where $\|r_i(t)\| = \|v_{i+1} - v_i\|$ and $e_i = \|r_i(t)\| - l_i$,

$$Rigidity\ Force : \beta_i = b_i \left(v_i - \frac{1}{2}(v_{i-1} + v_{i+1}) \right). \tag{3}$$

$$Normal\ Force : F_i = k_i\,(sign_i)\,n_i, \tag{4}$$

$$Image\ Force : f_i = \gamma_i \nabla P, \tag{5}$$

where n_i is the normal at the snaxel v_i and b_i, k_i, γ_i are force scale factors, $P = -\|\nabla I\|^2$, $sign_i = 1$ if $I(v_i) \geq T$ and $sign_i = -1$ otherwise (T is a thresholded for the image I). Region based statistics can be also used [13].

The T-Snake position is updated according to the following evolution equation:

$$v_i^{(t+\Delta t)} = v_i^t + h_i \left(\alpha_i^t + \beta_i^t + F_i^t + f_i^t \right), \tag{6}$$

where h_i is an evolution step.

The T-Snakes model incorporates also an *entropy condition*: "once a node is *burnt* (passed over by the snake) it stays burnt " [13, 12]. A termination condition is defined based on the number of deformations steps (*temperature*) that a triangle remains as a boundary one. A T-Snake is considered to have reached its equilibrium state when the temperature of all the snaxels fall below a pre-set "freezing point".

The T-Snake model can be summarized as follows [13, 12]. Until the temperature of all snaxels fall bellow the freezing point: Compute the external and internal forces and update the snaxels positions using equation (6). Compute the intersection between the grid and the model elements. Next, update the characteristic function (1) and through it determine the corresponding set of boundary triangles. For each boundary triangle find a model element which separates the inside from the outside nodes. Discard the other ones.

3 Original Dual-T-Snakes Algorithm

In this section we outline the basic points of the Dual-T-Snakes method [6]. The key idea behind this method is to explore the T-Snake framework to propose a *generalized Dual Active Contour Model* (Dual ACM) [6]: one T-Snake contracts and splits from outside the targets and another ones expand from inside the targets. The snake model is that one of section 2.1.

To make the outer snake to contract and the inner ones to expand we assign an inward normal force to the first and an outward normal force to the others according equation

(4). Also, to turn the T-Snakes evolution interdependent we use the *image energy* and an $affinity$ restriction.

We use two different definitions for image energy: one for the outer contour ((E_{outer})) and another one for the set of inner contours enclosed by it ((E_{inner})):

$$E_{outer} = \sum_{i=0}^{N-1} \left(- \|\nabla I(v_i)\|^2 \right) / N, \tag{7}$$

$$E_{inner} = \frac{1}{m} \left(\sum_{k=0}^{m} \left(\sum_{i=0}^{N_k-1} \left(- \|\nabla I(v_i)\|^2 \right) / N_k \right) \right), \tag{8}$$

where m is the number of inner curves.

If $E_{inner} > E_{outer}$ an inner curve must be chosen. To accomplish this we first use an $affinity\ operator$ which estimates the pixels of the image most likely to lie on the boundaries of the objects. Based on this operator, we can assign to a snaxel the likelihood that it is close to a boundary. That likelihood is thresholded to obtain an $affinity\ function$ that assigns to the snaxel a 0-1 value. Then the inner curve with highest number of snaxels with affinity function not null is chosen. If $E_{outer} > E_{inner}$ the outer snake is evolved if the affinity function corresponding is not null.

Also, the balance between the energy/affinity of the outer and inner snakes allows to avoid local minima. For instance, if a T-Snake has been frozen we can increase the normal force at the snaxels where the affinity function is zero.

To evaluate similarity between two contours we use the difference between the Characteristic Function of the outer snake and the Characteristic Functions of the inner ones ($Characteristic\_Diff$). For example, in the case of the CF triangulation of the Figure 1 we can stop the motion of all snaxels of an inner snake inside a triangle σ if any of its vertex $v \in \sigma$ has the two following properties:

Property (a). All the 6 triangles adjacent to v have a vertex where $Characteristic\_Diff = 0$*;*

Property (b). One of these triangles is crossed by the outer contour.

The freezing point is used to indicate that a T-Snake found an equilibrium position. In the following algorithm we call *Dual Snake* a list of T-Snakes where the first one is an outer contour and the others are inner contours. The algorithm can be summarized as follows:

Dual − T − Snakes Algorithm. Put all the dual snakes into a queue. Until the queue is empty do: Pop out a dual snake from the queue. Use the energies (equations (7) and (8)) and the affinity function to decide the snake to be processed. If all snaxels of that snake are frozen increase the normal force at those with affinity zero until the snake energy starts decreasing. Then, remove that added normal force and leave it to evolve until the temperature of all snaxels falls bellow the freezing point again. Analyze the $Characteristic\_Diff$ to identify if the snake being processed is close to a snake of the other type (inner/outer). In this case, remove the dual snake from the queue. Otherwise, mount the resulting dual snake(s) and go to the beginning.

4 Segmentation Framework

The Dual-T-Snakes method plus DP result in a boundary extraction procedure composed of four steps [7]: (a) The user defines seed points inside the objects and initializes the outer snake; (b) Computation of the Affinity operator and affinity function; (c) Application of the Dual-T-Snakes Algorithm; d) Find the final boundaries using Dynamic Programming.

As each boundary is enclosed by a dual snake (see Figure 4.b) the Viterbi algorithm [8] is suitable. In this algorithm the search space is constructed by discretizing each curve in N points and establishing a matching between them. These points are then connected by segments which are subdivided in M points to provide a *discrete search space* with NM points.

The energy functional used is given by [8]:

$$E_{snake} = \sum_{i=0}^{N-3} E_i \tag{9}$$

where:

$$E_i = \alpha E_{int}(v_i, v_{i+1}, v_{i+2}) + \beta E_{ext}(v_{i+1}) + \lambda E_{linha}(v_{i+1}), \tag{10}$$

with E_{int}, E_{ext} e E_{line} given by:

$$E_{int}(v_i, v_{i+1}, v_{i+2}) = \left(\frac{v_{i+2} - 2v_{i+1} + v_i}{\|v_{i+2} - v_i\|} \right)^2, \tag{11}$$

$$E_{ext}(v_i) = - \|\nabla I(v_i)\|^2, \tag{12}$$

$$E_{linha}(v_{i+1}) = \pm I(v_{i+1}). \tag{13}$$

with α, β and λ parameters to be chosen in advance.

The corresponding recurrence relation is the classical one given by [1]:

$$S_{i+1}(v_{i+2}, v_{i+1}) = \min_{v_i} \{ S_i(v_{i+1}, v_i) + E_i \}, \tag{14}$$

where E_i was defined just above.

5 Technical Details and Improvements

In this section we discuss some limitations of the original Dual-T-Snakes model (section 3) The solutions proposed are the main contribution of this paper.

5.1 Parameters Choise

For deformable modes, in general, the most commonly used method to set parameters is trial and error. You repeatedly modify the parameters and evaluate the result. Few works have been done to calibrate parameters automaticaly [15]. This point is critical for Dual-T-Snakes as we have both the outer and inner snakes to calibrate.

Such as the T-Snakes model, the parameters of the original Dual-T-Snakes method are the stiffness parameter a_i, the natural length l_i, the rigidity b_i, the normal force parameter k_i and the external force scale γ_i.

The Figure 2.a shows the difficulties in this case. In this figure we picture a sequence of snaxels for the outer and inner snakes. The elastic and the rigidity force are represented following the expressions (2)-(3), respectively. We are supposing that the natural length l_i is zero and that the image forces can be discarded (low contrast). The difficulty is that for the outer snake the elastic and rigidity forces point towards the boundary while for the inner snake these forces point in a oposite direction.

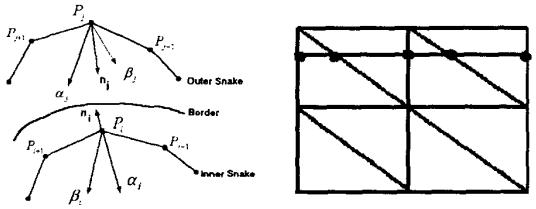

(a) (b)

Figure 2: (a)Internal forces for Dual-T-Snakes. (b)Effect of reparameterization over snaxels distribution.

The problem behind this behavior is the choise of the normal force parameter. In fact, it should be high enough to make the internal T-Snake to evolve in the desired direction but, if it is too high, the internal forces of the outer snake may be so strong that we may lost the boundary.

To address this difficult we could set different values for the inner and outer snakes. However such idea implies to calibrate two unrelated snakes which is an undesireble task.

The elastic force also depends on the natural length l_i. The role of this parameter is to bias the distribution of snaxes into an uniform one. However, in the Dual-T-Snakes model the reparameterization is done through the projection over the triangulation. So, a curve with uniform distribution of snaxel may have non-uniform distribution after the reparameterization (see Figure 2.b).

From these remarks, we decided to simplify the model (6) by setting l_i and a_i to zero. Thus we still have the effect of reducing curvatures of the rigidity forces and discard natural length parameter whose effects are not worthwhile for the model. However, the problem pictured on Figure 2.a remains. It will be addressed again on section 5.2 bellow. The final model to be used is given by:

$$v_i^{(t+\Delta t)} = v_i^t + \frac{\Delta t}{\gamma}\left(\beta_i^t + F_i^t + f_i^t\right). \qquad (15)$$

5.2 Image and Normal Forces

Another point is that the normal force definition given by the equation (4) is limited for noise images because it may implies in many oscilations of the snake due to the abrupt variantions of image intensity (Figure 3.a). This may lead to instabilities and performance problems as the number of deformation steps may be too large due to the oscilations.

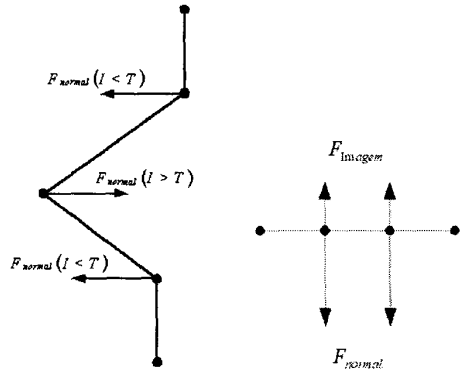

(a) (b)

Figure 3: (a)Normal force generates local oscilations. (b)Null Internal forces due to snaxels alignmen.

In this paper, we address these problems by proposing a new definition for the normal force as follows:

$$F_i(v_i) = Val(v_i)\, kn_i, \qquad (16)$$

where $Val(v_i) = 1$ if $I(v_i) < T$, $Val(v_i) = 0$ otherwise. Also, n_i, k and T have the same meaning then in the equation (4).

With this definition, we can reduce the oscilations by avoiding situations like on Figure 3.a. On the other hand, we still have the effect of pushing the snake towards the object boundary. Despite this, the snake may be frozen far way the desired region. However, the tests demonstrate that the number of times that this happens is reduced dramaticaly, mainly for noise images, which is the desired effect.

In a simple way, definition (16) implies that we are using the normal force only to get closer the region of interest. Thus we can set the normal force large enough to solve the problem pictured on Figure 2.a without making the outer

snake passes over the target. When close the bounday, the normal force will be null and the equilibrium depends only on the external and rigidity forces. This is another advantage of the definition (16) because we avoid the subtle trade-off between the normal end image forces observed for example, in the Balloon model [4]. However, the smoothness of the final result may be affected. This is discussed bellow.

5.3 Smoothing Forces

Some considerations should be done about the smoothness of the result obtained with definition (16). So, let's see Figure 3.b. In this Figure we have a sequence of snaxels in line and uniformly distributed. In this case, the rigidity force given by equations (3) is null.

So, in this case, the resultant force over each snaxel is given by the normal force plus the image force. However, if the snake is near a boundary then the normal force may be null due to the definition (16) and we will have only the image force over each snaxel. This lack of internal forces may implies less smoothoness for the final result, which is an undesirable effect of the definition 16.

However, for the Dual-T-Snakes model this behaviour is not critical as the method is used only to reduce the search space. The tests have shown that this lack of smoothness is not critical for the DP step. Besides, the local oscilations observed change the temperature of the snaxels until them fall below the freezing point. Hence, the stoping criterium of the T-Snakes remains efficient.

5.4 Avoiding Local Minima

In the original Dual-T-Snakes model, we propose to increase the normal force for snaxels with affinity zero to push a T-Snake away from local minima. This method can be efficient for images with artefacts. However, for noise images this methodology implies in instabilities as the normal force depends on the image threshod (Figure 3.a).

In this paper we propose other three methods: (1) Relax the image threshold T in equation (4) (section 6.1); (2) A Multigrid approach (section 6.3); (3) A Region Growing method based on the grid (section 6.4).

6 Experimental Results

In this section we present results for 2D images obtained through the segmentation framework of section 4 with the improvements proposed above.

The discussions bellow are steered by the following aspects: (a)Computational cost; (b)Model parameters and noise; (c)Efficience of the new normal force definition (equation 16); (d)Methods to get a T-Snake to go away from a local minimum.

During a deformation step, each snaxel moves some distance D according to the equation (15). Following Gunn and Nixon in their Dual ACM [8], we decided to stablish a maximum D allowed (one pixel in general). Thus we can improve the numerical stability as well as guarantee the efficience of the image energy definitions (7)-(8).

Snake models are in general applied after some kind of image processing methods for noise reduction and edge detection [10]. We demonstrate bellow that hierarchical filtering and directional smoothing can be usefull in the segmentation framework proposed.

6.1 Synthetic Images

In the following examples we start from the image on Figure 4.a and increase the gaussian noise ($mean = \mu$ and $variance = \sigma$) as indicated on Table 1. The grid resolution is 5×5 for all examples corresponding. The Dual-T-Snakes parameters are also indicated on that Table.

μ,σ	k	γ	b	$Snake0$	$Snake1$
30.0 , 5.0	200.0	50.1	50.0	40	97
30.0 , 10.0	200.0	50.1	50.0	41	89
50.0 , 25.0	200.0	50.1	50.0	38	112
50.0 , 40.0	200.0	50.1	50.0	43	149

Table 1: From left to right: mean,variance,Dual-T-Snake paramenters,num. of deformation steps for Snake 0 and for Snake 1.

It is difficult to compare results about the computational cost of snake models due to the lack of such results in the literature. However, from the Figure 4.a we can realise that the distance between the inner snake (Snake 1) and the interested boundary has an upper bound of order 45 pixeis. If considering the last image ($\mu = 50.0$,$\sigma = 40.0$), we consider that the number of interactions is acceptable.

The Figures 4.b shows a tipical Dual-T-Snakes results for this set of images. The first aspect to be considered is the distance between the inner and outer snakes in some regions of Figure 4.b.

This behavior is due to the terminating criteriun given by properties (a)-(b) of section 3. These "defects" do not affect the Viterbi result, unless we use a too coarse grid resolution [5].

It is opportune to compare the performance if we use the normal force of the original Dual-T-Snakes given by equation 4. By using the new definition (equation (16)), the inner snake gets the final result with 149 interactions (Table 1) while by appling the original one (equation 160) the inner snake did 168 interactions but it is still far away from boundary (Figure 4.d).

From Table 1 we can observe that parameters do not change when the noise was increased. This indicates stabil-

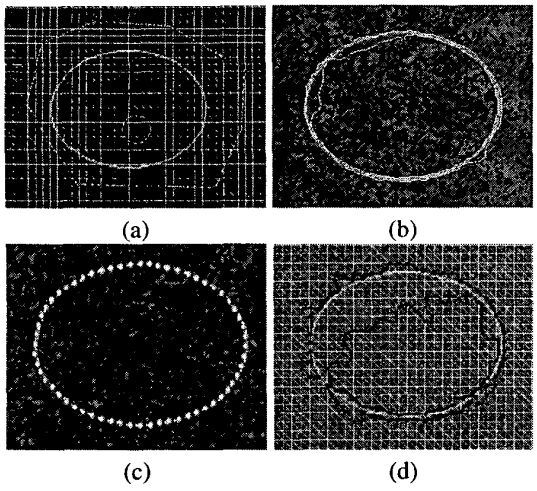

Figure 4: (a)Initial image and initialization. (b)Dual-T-Snakes result for 5×5 grid. (c)Viterbi result. (d)Interaction 168 with original Dual-T-Snake model.

ity of the parameters over noise which is a desired feature for the model. Also, we use the method (1) of section 5.4 to go away from a local minimum; that is: $T \rightarrow (T \pm \Delta T) \in (\mu - \sqrt{\sigma}, \mu + \sqrt{\sigma})$.

Figure 4.c shows a tipical Viterbi solution for the examples of this section. The parameters used for all of them are: $\alpha = 1200.0, \beta = 0.5$ and $\lambda = 140.0$. Hence, the Viterbi parameters show also stability under noise variation. More tests can be found in [5]. All of them indicating the same behaviour.

6.2 Blood Cells

The following example is usefull to understand how multi-scale methods fits very well with our segmentation framework. The Figure 5.a shows a blood cell obtained by an electronic microscope technique. When pass-band filter is applied, we get an edge map resembling a ribbon whose thickness depends on the kernel size of the filter used (Figure 5.b). That is an ideal situation for applying Dual-T-Snakes plus Viterbi because first the former extracts the ribbon (Figure 5.c). Then the later may be applied to the original image to give the final result (Figure 5.d).

6.3 Electronic Micrography of Nucleolus

In this example we will show how the Dual-T-Snakes can be used in a multigrid methodology.

Let's take the Figure 6.a which pictures an image of a cell nucleolus whose resolution is 895×682.

We can observe the presence of noise and artefacts as

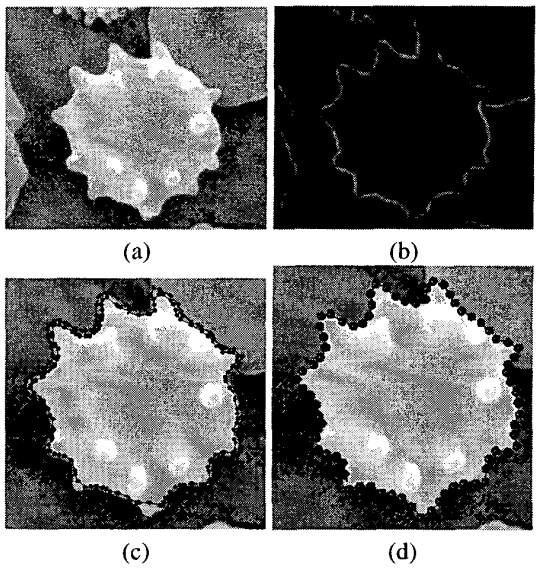

Figure 5: (a)Image to be processed. (b)Band-Pass filtered image. (c)Dual-T-Snakes solution. (d)Viterbi solution.

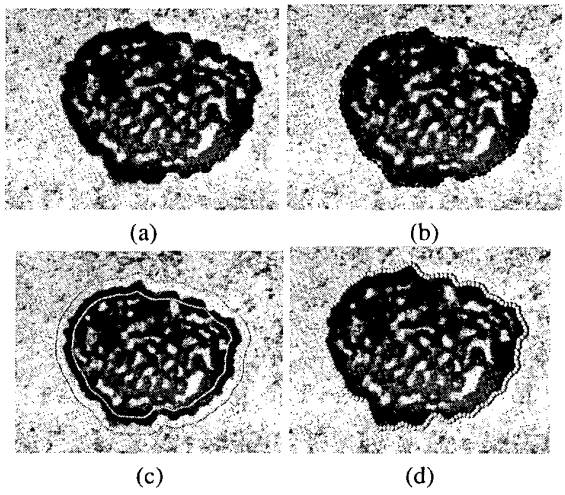

Figure 6: Segmentation of nucleolus: (a)Original image. (b)Partial solution. (c) Offsets of partial solution. (d)Extracted boundary.

well as that the interested boundary have points with high curvature.

To be able to extract the boundary details we have to use a grid with enough resolution [13]. However, the finner is the grid resolution the stronger is the effect of the noise and artefacts [5]. On the other hand, a coarse grid resolution could lost details in points with high curvature.

This drawback can be addressed in the Dual-T-Snakes framework by a multigrid approach based on the following steps: (1)Apply Dual-T-Snakes for a coarsest resolution and the Viterbi algorithm next; (2)Offsets of the result obtained; (3)Dual-T-Snakes for a finner grid followed by Viterbi to get the final result.

Figures 6.b shows the result of step (1) with the following parameters: $k = 200.0$, $\gamma = 50.0$, $b = 10.0$, $T = 140.0$, *Freezing Point*= 15 and grid resolution 15×15. The max step allowed in each interaction is 2 pixels. The Viterbi result (Figure 6.b) was obtained with the following parameters: $\alpha = 1200.0, \beta = 0.5$ and $\lambda = 0.0$.

The distance between an offset and the partial solution is of order of the grid resolution. Hence, we should apply Dual-T-Snakes again in the last step to get a more reduced search space as the distance between the offsets is of order 30 pixels in this case (Figure 6.c). Figures 6.d shows the final result of step (3) with the some parameters values above.

6.4 Electronic Micrography of Cat Cells

The next example uses topological changes in the context of cell images. Figure 7.a shows the original image whose resolution is 600x600. In this case particularly, the image has artefacts, structures and textures which may stop the snake evolution far away from the cells.

An importante observation is that the grey level intensity of the cell boundaries is of order $T = 80.0$. Linear scalespace methods will mix the boundary with its neighboorhods given problems to extract the boundary in the coarse scale.

Non-linear methods could be better. In this case, we use directional smoothing. A more sophisticate one could be non-linear diffusion [5]. Figure 7.b shows the filtered image and the Dual-T-Snakes initialization is presented. The (partial) solution is shown on Figure 8.a. The parameters values are: $k = 200.0$, $\gamma = 50.0$, $b = 10.0$, $T = 80.0$, *Freezing Point*= 28 and grid resolution 20×20.

At first, the method used to push a T-Snake away from a local minimum is to relax the threshold. The normal force definition is given by equation (16).

This example shows a difficulty for the original proposal of the Dual-T-Snakes: in the presence of big artefacts, the terminating criterium of section 3 may never hold. That is exactly what is happening in this case. This example

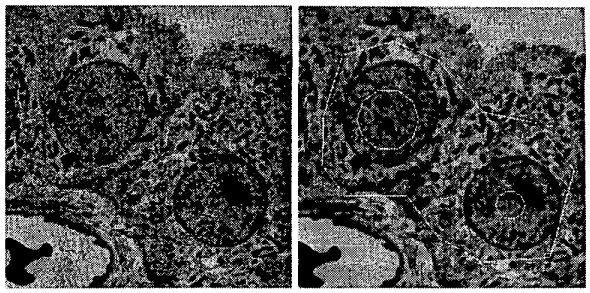

(a) (b)

Figure 7: (a)Initial image. (b)Filtered image and Dual-T-Snakes initialization.

shows also the necessity of an upper bound of interactions to avoid an infinite loop. For example, a multiple of the freezing point.

The main problem about the botton right cell is that the threshold that characterizes the boundary holds also for a structure in its interior (Figure 7.a). The solution proposed to address this problem can be visualized on Figure 8.b: firstly, we mark the grid nodes interior to the inner snake as well as its neighboors ones whose grey intensity is above the threshold; next, we get a piecewise linear curve through a simple continuation algorithm ([5]).

The method is a kind of region growing and the obtained curve can be used to re-initialize the Dual-T-Snakes for that cell (Figure 8.b). The corresponding Dual-T-Snake solution is shown on Figure 8.c. Now, the terminating criterion is satisfied. The Viterbi solution is presented on Figure 8.d. The parameters used in this fase are: $\alpha = 1200.0, \beta = 10.0$ and $\lambda = 20.0$.

7 Future Works and Conclusions

The segmentation method based on Dual-T-Snakes plus the Viterbi algorithm can be applied together with a non-parametric multiscale methodology based on the following steps: (1)Pyramid model; (2)Solve Dual-T-Snakes plus Viterbi for the coarsest resolution; (3)Track the Virterbi Solution through the pyramid following [14].

Anther possibility would be to use linear multiscale methods [10] to construnt the pyramid model. Than, Dual-T-Snakes is applied in the coarsest scale and the solution obtained is used to initialize the Dual-T-Snakes in a finner one. The method proceed until the terminating criterium is reached. Than, Viterbi algorithm is applied in the finnest scale.

The improvements proposed on section 5 for the original Dual-T-Snakes (parameters, normal force definition, methods to avoid local minima) allow this method to be applied more eficiently as we demonstrated in the experi-

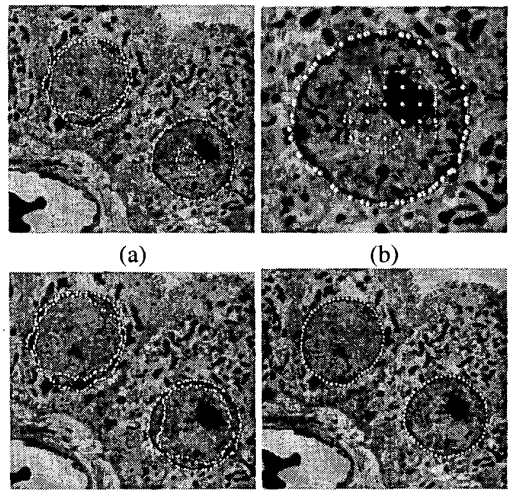

Figure 8: Segmentation of Cat cells. An example using topological changing capabilities.

mental results.

8 Acknowledgments

We would like to acknowledge CNPq for the financial support for this work.

References

[1] A. A. Amini, T. E. Weymouth, and R. C. Jain. Using dynamic programming for solving variational problems in vision. *IEEE Trans. on Pattern Analysis and Machine Intel.*, 12(9):855–867, September 1990.

[2] P. Bamford and B. Lovell. A two-stage scene segmentation scheme for the automatic collection of cervical cell images. In *Proceedings of TENCON '97, Brisbane, Australia.*, December 1997.

[3] A. Black and A. Yuille, editors. *Active Vision*. MIT Press, 1993.

[4] L. D. Cohen. On active contour models and balloons. *CVGIP:Image Understanding*, 53(2):211–218, March 1991.

[5] G. A. Giraldi. *T-Snakes Duais e Inicialização de Modelos Deformáveis*. PhD thesis, Departamento de Engenharia de Sistemas e Computação - COPPE - UFRJ. Web Site (In portuguese): http://virtual01.lncc.br/ giraldi/Tese/index.html, 2000.

[6] G. A. Giraldi, L. M. Gonçalves, and A. F. Oliveira. Dual topologically adaptable snakes. In *Proceedings of the Fifth Joint Conference on Information Sciences (JCIS'2000, Vol. 2) - Third International Conference on Computer Vision, Pattern Recognition, and Image Processing*, pages 103–106, 2000.

[7] G. A. Giraldi, E. Strauss, and A. F. Oliveira. A boundary extraction method based on dual-t-snakes and dynamic programming. In *IEEE Computer Society Conference on Computer Vision and Pattern Recognition (CVPR'2000)*, 2000.

[8] Steve R. Gunn. *Dual Active Contour Models for Image Feature Extraction*. PhD thesis, Faculty of Engineering and Applied Science, Department of Eletronics and Computer Science., May 1996.

[9] M. Kass, A. Witkin, and D. Terzopoulos. Snakes: Active contour models. *International Journal of Computer Vision*, 1(4):321–331, 1988.

[10] F. Leymarie and M. D. Levine. Tracking deformable objects in the plane using and active contour model. *IEEE Trans. Pattern Anal. Mach. Intell.*, 15(6):617–634, June 1993.

[11] T. McInerney and D. Terzopoulos. Topologically adaptable snakes. In *Proc. Of the Fifth Int. Conf. On Computer Vision (ICCV'95), Cambridge, MA, USA*, pages 840–845, June 1995.

[12] T. McInerney and D. Terzopoulos. Topology adaptive deformable surfaces for medical image volume segmentation. *IEEE Trans. on Medical Imaging*, 18(10):840–850, October 1999.

[13] T. J. McInerney. *Topologically Adaptable Deformable Models for Medical Image Analysis*. PhD thesis, Department of Computer Science, University of Toronto, 1997.

[14] M. Mignotte and J. Meunier. An unsupervised multiscale approach for the dynamic contour-based boundary detection issue in ultrasound imagery. In *Proceedings of the Fifth Joint Conference on Information Sciences (JCIS'2000, Vol. 2) - Third International Conference on Computer Vision, Pattern Recognition, and Image Processing*, pages 366–369, February, 2000.

[15] J. M. Carstensen R. Fisker. On parameter estimation in deformable models. In *14th International Conference on Pattern Recognition*, pages 762–766, August 16-20 1998.

[16] Gang Xu, E. Segawa, and S. Tsuji. Robust active contours with insensitive parameters. *Pattern Recognition*, 27(7):879–884, January 1994.